Bulletin de l'Institut Scientifique, Rabat,
section Sciences de la Terre, 2006, n°28, 19-30.

Special paper : Colloque séisme d'Al Hoceima
Al Hoceima 24-26 février 2005

Focal mechanisms and state of stress in the Al Hoceima area (Central Rif, Morocco)

Fida MEDINA[1] & Sidi Otman EL ALAMI[2]

1. Université Mohammed V–Agdal, Institut Scientifique, Département de Géologie, B.P. 703 Agdal, Rabat, Maroc. e-mail : medina@israbat.ac.ma
2. Université Mohammed V–Agdal, Institut Scientifique, Département de Physique du Globe, B.P. 703 Agdal, Rabat, Maroc. e-mail : elalami@israbat.ac.ma

Abstract. The review of the available focal mechanisms of the Al Hoceima area for the period 1968-2004 shows that: (1) most mechanisms correspond to normal and/or strike-slip faulting mainly. The state of stress determined with the help of the numerical quadridimensional search (R4DT) for three sets of earthquakes (single events, 1994 and 2004 crises) shows that the main compressional axis σ_1 is NNW-SSE, while the minimum compressional stress axis σ_3 is ENE-WSW in the three cases; (2) focal mechanisms are homogeneous by event (main shock and its aftershocks), but become heterogeneous when corresponding to single events which are time- and space-distant, reflecting the structural diversity of the area. The NW-SE trend of the main compressional stress axis agrees with the displacement vector of Africa with respect to Eurasia in the area, with local variations. The obtained states of stress correspond to the regional state of stress for moderate earthquakes (M ≥ 4) and to local states of stress for the weak events.

Mécanismes au foyer et état de contrainte dans la région d'Al Hoceima (Rif central, Maroc).

Résumé. La revue des mécanismes au foyer disponibles pour la région d'Al Hoceima durant la période 1968-2004 montre que : (1) la plupart des mécanismes correspondent à des failles normales et/ou décrochantes principalement ; l'état de contrainte déterminé à l'aide de la méthode numérique de recherche quadridimensionnelle (R4DT) pour trois groupes de séismes (événements isolés et crises sismiques de 1994 et 2004) montre que la direction de l'axe de la contrainte compressive maximum σ_1 est NNW-SSE, celle de la contrainte compressive minimum étant ENE-WSW ; (2) les mécanismes au foyer sont homogènes par événement (séisme principal et ses répliques) et hétérogènes quand ils sont isolés et temporellement et spatialement distants, reflétant la grande diversité structurale de la région. La direction NW-SE de la contrainte compressive maximale est compatible avec le vecteur déplacement de l'Afrique par rapport à l'Eurasie dans la région, avec des variations locales. Les états de contrainte obtenus correspondent à l'état de contrainte régionale pour les séismes modérés (M ≥ 4) et à des états de contrainte locaux pour les séismes faibles.

INTRODUCTION

Al Hoceima city is located in the northern part of the Rif chain, a region which has been suffering the largest seismic activity in Morocco (Fig. 1), as also shown by the earliest earthquake catalogues for this country (see Cherkaoui 1988, for a list of catalogues) and by the historical studies (Elmrabet 2005). In this area, earthquakes are frequent, shallow (z < 30 km), and of moderate magnitude (M < 5), with the exception of the 26 May 1994 and 24 February 2004 shocks, which attained magnitudes Md = 5.6 and Mw = 6.3 respectively.

On the scale of the Betic-Rif Arc, seismicity appears to be largely scattered (e.g. Udias *et al.* 1976, Cherkaoui 1988, El Alami *et al.* 2004) ; however, at the regional scale, epicentres of some well-constrained aftershocks are clearly aligned along NNE-SSW, NNW-SSE and WNW-ESE trends (Cherkaoui *et al.* 1990, Calvert *et al.* 1997, El Alami *et al.* 1998, Dorbath *et al*. 2005, Buforn *et al.* 2005). On a more global scale, seismicity of northern Morocco is related to the N320°E-trending relative convergence of the African and Eurasian plates, with a theoretical velocity of 0.5 cm/yr according to models NUVEL-1 et NUVEL-1A (DeMets *et al.* 1994). The 'instantaneous' smaller rates of 0.06 cm/yr recently suggested by Buforn *et al.* (2004) from seismicity, are explained by the lack of major earthquakes during the 20th century.

On the base of focal mechanisms data, determination of the state of stress using the right dihedra method (Angelier & Mechler 1977, Allmendinger *et al*. 1989), and/or numerical methods (e.g. Carey & Brunier 1974, Angelier & Goguel 1979, Etchecopar *et al.* 1981, Rivera & Cisternas 1990) was attempted in the region. These methods have been applied to microseismicity of the Al Hoceima area during 1989 (Medina 1995), and to the seismic crises of 1994 (El Alami *et al.* 1998) and 2004 (Dorbath *et al.* 2005).

This paper exposes a review of the focal mechanisms determined up to 2004 for the earthquakes of the Al Hoceima region (34.5°-35.6°N; 3.5°-4.25°W), and a new approach of the related state of stress, mainly based on the numerical search method R4DT (Angelier 1990).

GEOLOGICAL SETTING

Al Hoceima is located in the central Rif chain, which parallels the northern coast of Morocco (Fig. 2). Near the city, the most important structures consist of southward-verging thrust sheets which are, from the upper (northernmost) to the lower (southernmost): (i) the Bokkoya, with nappes of Palaeozoic terranes and their Mesozoic-Cenozoic cover; (ii) the Tiziren unit, comprising Middle Jurassic to Early Cretaceous carbonates and flysch series (3000 m); (iii) the Ketama metamorphic unit, which consists of Cretaceous flysch and limestones. Volcanic rocks are represented by the middle Miocene Ras-Tarf andesites (Guillemin & Houzay 1982).

Recent sediments (Miocene and younger deposits; Thauvin 1971) overlying the previous units are encountered in the triangular lower Nekor graben, trending N-S, and the Boudinar basin, east of Ras Tarf Cape.

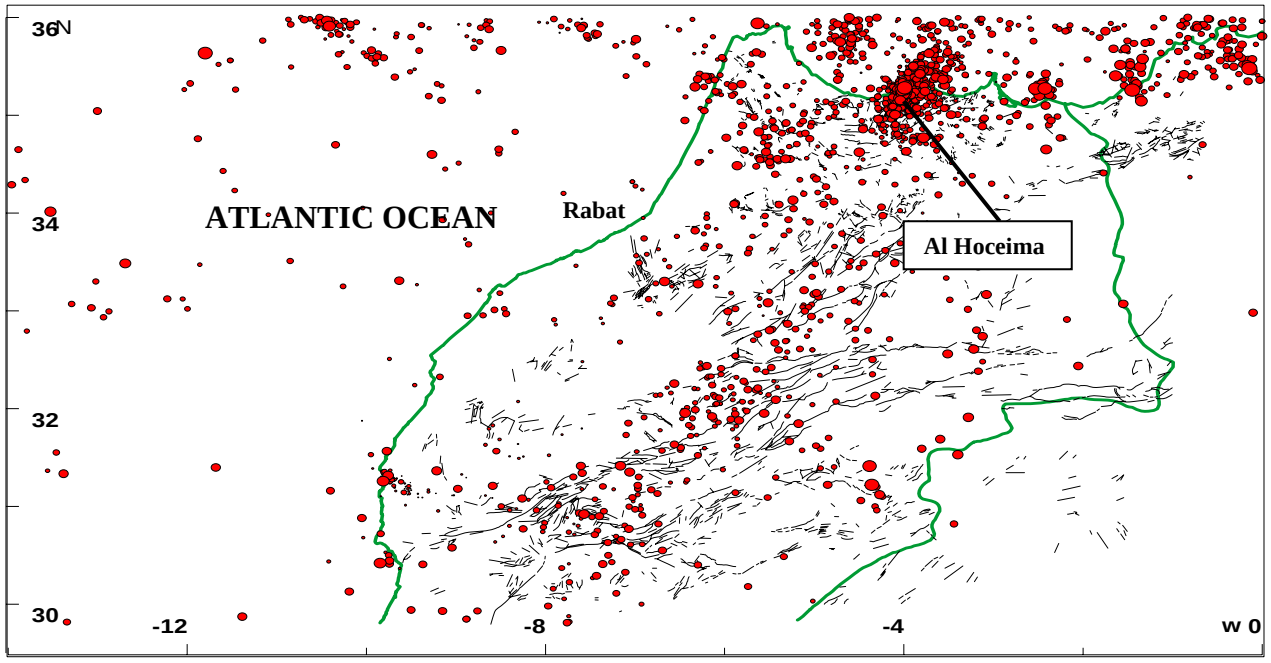

Figure 1. Seismicity of Morocco (northern provinces) for the period 1987-2000 (files El Alami) and main fault structures. Symbols correspond to epicentres of earthquakes. The size of symbols increases with increasing magnitudes.

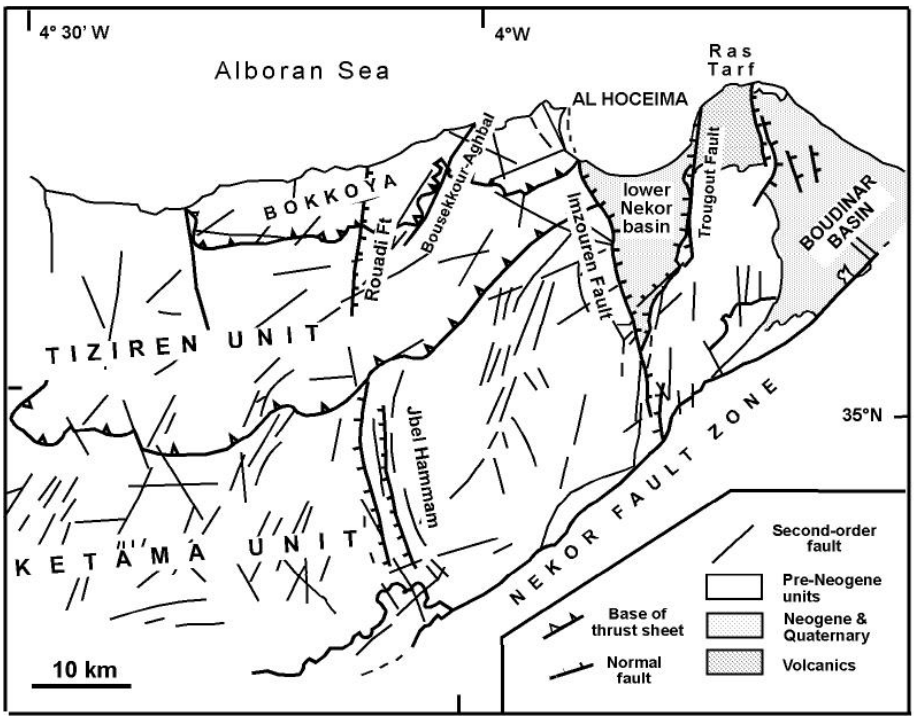

Figure 2. Structural map of the Al Hoceima area and main faults; after several authors (cited in Medina 1995).

In addition to the Nekor fault, which is the major transverse structure (e.g. Leblanc & Olivier 1984), the most important faults are:

(i) The Imzouren (NNW-SSE) and Trougout (N-S) normal faults, which respectively delimit the western and eastern boundaries of the lower Nekor graben; the Trougout fault is thought to extend offshore into the Al Hoceima Bay (Calvert *et al*. 1997).

(ii) The Jbel Hammam fault system (NNW-SSE), consisting of several normal faults with trace lengths of 20 km.

(iii) The Rouadi fault, a normal fault trending NNE-SSW over 15 km, the eastern block is downthrown.

(iv) The Bousekkour-Aghbal strike-slip fault (Fig. 2), trending NE-SW, which crosscuts the whole Bokkoya unit with a sinistral displacement (Mourier 1982). This fault is thought to have been active during the 1994 seismic crisis (El Alami *et al.* 1998).

Most authors agree that, after the pre-Messinian emplacement of the Rif nappes, the tectonic regime was dominated by simultaneous normal and strike-slip motion along the faults. Normal faulting generally takes place on fault planes parallel to the compressional stress axis, whereas strike-slip motion is observed on the planes which are at a certain angle with the compressional stress axis. Structural analysis carried out by Frizon de Lamotte (1982, p. 297) and Chotin & Aït Brahim (1988) shows that horizontal σ_1 underwent a counterclockwise rotation: ENE-WSW during the Tortonian, NNE-SSW during the end-Tortonian, and NW-SE in the Plio-Quaternary, even though a more complex evolution involving extensional episodes is inferred from local studies (Groupe de Recherche Néotectonique de l'Arc de Gibraltar 1977).

REVIEW OF THE FOCAL MECHANISMS OF THE AL HOCEIMA AREA

A large number of focal mechanisms were determined for the Al Hoceima area since the 1970's. Solutions were first obtained using first motion polarities of P-waves, and, more recently, waveform analysis and moment tensor inversion (Table I).

Because of the large population of focal mechanisms, it is easier to represent them by their tectonic axes *P, T* and *B* within triangular diagrams (Frohlich & Apperson 1992). This representation, already used for the studied area (Medina 1995, Buforn *et al.* 2004), helps directly determining the tectonic regime. Besides the triangular diagrams, azimutal scatter of axes *P* and *T* is visualised on classical equal-area stereograms.

The list of focal mechanisms used is given in Tables A – D of the Appendix.

Table I. Methods and database used by previous authors for determining focal mechanisms of the Al Hoceima area.

Method	Authors	Events
Polarity of P-wave arrivals	Hatzfeld (1978)	teleseisms previous to 1980
	Medina & Cherkaoui (1992)	teleseisms 1959-1986
	Hatzfeld *et al.* (1993)	microseisms of 1989
	Medina (1995)	microseisms of 1989, teleseisms
	El Alami *et al.* (1998)	major events of the 1994 seismic crisis
	Instituto Geografico Nacional (IGN, Spain)	teleseismic events
	Bezzeghoud & Buforn (1999)	teleseismic events
Waveform analysis	Bezzeghoud & Buforn (1999) and Buforn *et al.* (2005)	major shocks of 1994 and 2004
Moment tensor inversion	IGN and IAG, centres ZUR (Switzerland) and MED (France), Stich *et al.* (2003) and Rueda & Mezcua (2004)	moderate teleseisms (4<M<5)

Single events 1968-2001

Fifteen (15) focal mechanisms were determined for the single events recorded from 1968 to 2001 (Table A, Appendix), most of them corresponding to strike-slip displacements with normal component and to normal faults (Fig. 3). Few mechanisms correspond to strike-slip motions with reverse component. The left side of the diagram (*B*–*P*), shows a gap between strike-slip and normal mechanisms. On a stereographic projection, axes *P* are distributed in the NW and SE quadrants with variable plunge, with the exception of two axes located in the NE quadrant.

Microseismicity 1989

Three hundred and sixteen micro-earthquakes were recorded during the microseismic survey carried out during October–November 1989, of which 231 were accurately located (Cherkaoui *et al.* 1990, Hatzfeld *et al.* 1993). Plotting the axes of 88 determined mechanisms (Hatzfeld *et al.* 1993, Medina 1995, his Fig. 6) shows that the dominant regime is strike-slip/normal, with a general lack of pure reverse mechanisms. On a stereographic projection, axes *P* are distributed along a NW-SE great circle, with largely variable plunges, whereas axes *T* are NE-SW to ESE-WNW with a shallow plunge (Medina 1995, his Fig. 5).

1994 seismic crisis

Solutions obtained for the main event of the 1994 seismic crisis from moment tensor inversion (USGS, Harvard, CSEM) or from waveform modelling (Bezzeghoud & Buforn 1999) show strike-slip motion with a slight normal component (Fig. 4). The solution proposed by El Alami *et al.* (1998) on the base of first motions includes a reverse component (Table B, Appendix). Bezzeghoud & Buforn (1999) suggested that the main event consists of two sub-events, mechanism of sub-event 2 also showing a reverse component.

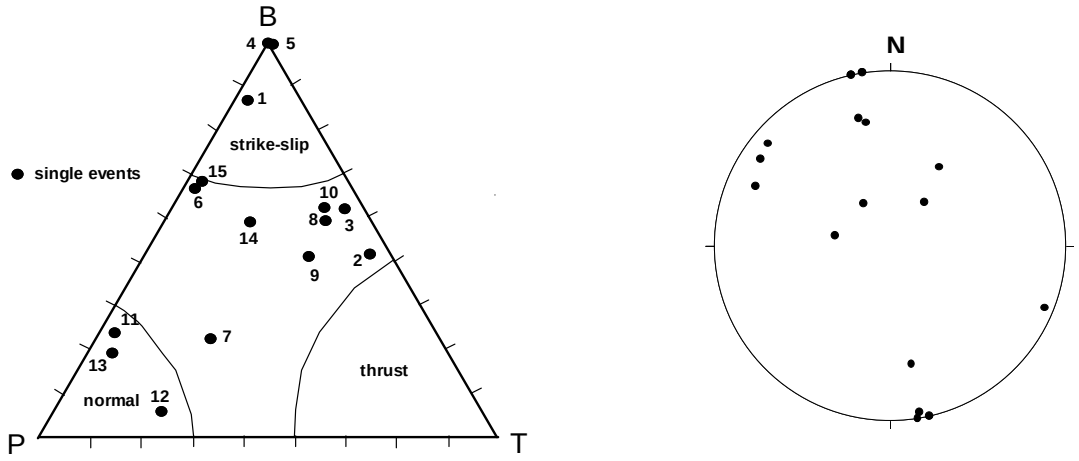

Figure 3. Left, distribution of the tectonic axes *P, B* and *T* (points) on a triangular diagram (Frohlich & Apperson 1992) for single events of the Al Hoceima area. Right, azimutal distribution of *P* axes on a stereographic projection (lower hemisphere) for the same events. The numbers correspond to events listed in Table A (Appendix).

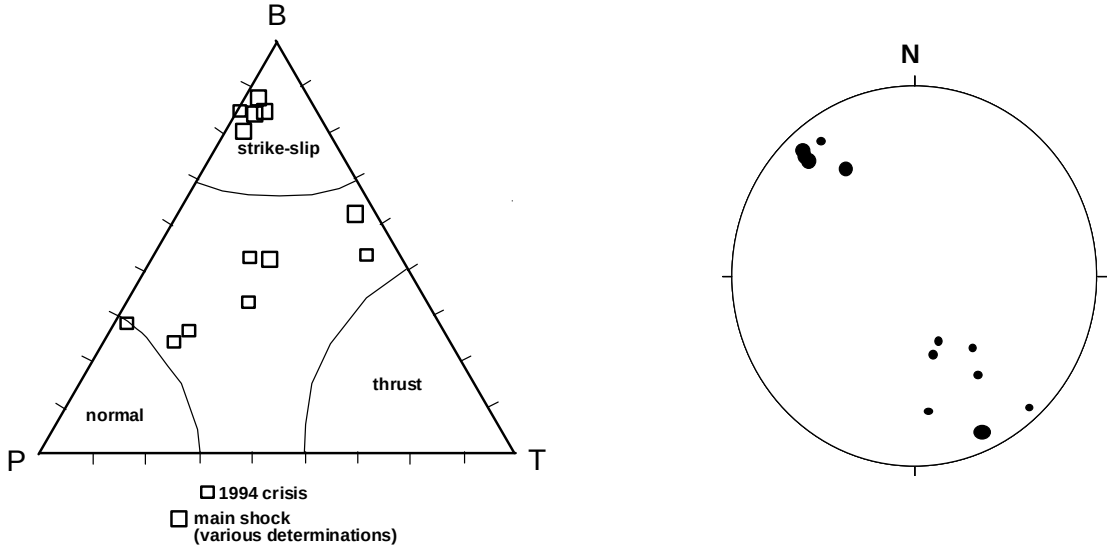

Figure 4. Distribution of the tectonic axes *P, B* and *T* (points) on a triangular diagram (Frohlich & Apperson 1992) for the main events of the 1994 crisis, and azimutal distribution of *P* axes on a stereographic projection (lower hemisphere) for the same events. Data from El Alami *et al.* (1998).

Mechanisms of the 7 main aftershocks (Tab. C, Appendix) all correspond to strike-slip motion with a normal component (El Alami *et al.* 1998; Fig. 4). On a stereographic projection, *P* axes are oriented NW-SE with a slight to moderate plunge.

2004 seismic crisis

For the main shock of 24 February 2004, focal mechanisms were determined from moment tensor inversion (USGS, Harvard, LDG) (Table D, Appendix). Nodal planes are oriented NNE-SSW and WNW-ESE with ESE and SSW steep dips respectively. Mechanisms of the strongest aftershocks, determined by IGN (Table E, Appendix) correspond to strike-slip faulting with a reverse component mainly, and to reverse faulting (Fig. 5). One single case shows normal faulting (mechanism 7).

Mechanisms of the weakest aftershocks also correspond to strike-slip faulting with mainly a normal component (Dorbath *et al.* 2005).

On a stereographic projection, axes *P* concentrate around azimut N330°E.

STATE OF STRESS

Methodology

An approach of the state of stress was attempted by several authors for northern Morocco, and particularly for the Al Hoceima area. The main methods used are listed in Table II.

In the present study, focal mechanism analysis was carried out with the help of software TENSOR, with

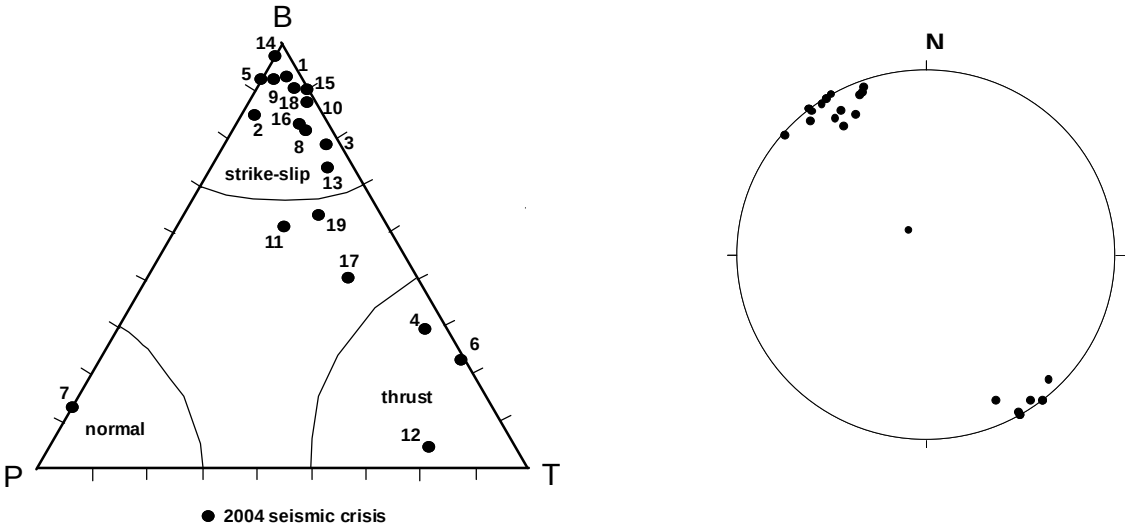

Figure 5. Distribution of the tectonic axes *P*, *B* and *T* (points) on a triangular diagram (Frohlich & Apperson 1992) for the main shock and aftershocks of the 2004 crisis, and azimutal distribution of axes *P* on a stereographic projection (lower hemisphere) for the same events. Data from IGN (Spain). The numbers correspond to events listed in Table E (Appendix).

Table II. Methods and database used by previous authors for determining the state of stress in the Al Hoceima area and Morocco.

Method	Author(s)	Events
Right diherdra method (Angelier & Mechler 1977)	Galindo-Zaldivar *et al*. (1993) and Henares *et al*. (2001)	teleseisms
	Medina (1995)	microseisms of 1989 and teleseisms
Numerical method R4DT (Angelier)	El Alami *et al.* (1998)	1994 earthquake and aftershocks
Numerical method (Rivera & Cisternas 1990)	Dorbath *et al*. (2005)	aftershock sequence of the 2004 earthquake (pers. comm..)

quadridimensional iterative search (R4DT) option (Angelier 1990). The state of stress is defined by the trend and plunge of the main stress axes ($\sigma_1 \geq \sigma_2 \geq \sigma_3$), and by their relative magnitude, expressed by ratio $\Phi = (\sigma_2-\sigma_3)/(\sigma_1-\sigma_3)$. After a preliminary determination involving both nodal planes of each focal mechanism, we selected for each solution the plane showing the least angular difference between the observed slip vector and the calculated shear stress (Carey-Gailhardis & Mercier 1987, Angelier 1990). Methodology is illustrated in Figure 6.

Reliability of solutions

The reliability of focal mechanism solutions used constitutes one of the main parameters on which is based the determination of the state of stress. In order to favour the most reliable mechanisms, the focal mechanism planes were weighted with respect to the quality of the solutions. The weight assigned to each plane depends on :

(1) The magnitudes of the corresponding shocks, so that the largest weights were assigned to the shocks with highest magnitudes ; this obeys to the fact that high magnitudes reflect large rupture parameters, such as the width, the length, the area, and the surface displacement (e.g. Wells & Coppersmith 1994).

(2) The number and distribution of stations on the diagram for solutions determined with the help of P-wave first arrivals. In this case, the assigned weight depends on the quality of the solution. Data which were not directly observed were given the minimum value, because no control was possible on the quality of the solutions.

In addition, the accuracy of the tensors was estimated by quality factors n_1 et n_2 which express the number of planes with angular differences ANG>45° and 22.5°<ANG<45° between the slip vector and the shear stress obtained.

Results

The following results were obtained (Table III; Fig. 7):

– For the 15 single events in the Al Hoceima area (period 1968-2001), the software excluded only mechanisms 2 and 12 (Appendix); the state of stress determined for 13 mechanisms is extensional, with almost-horizontal σ_3 plunging 3° towards N245°E, and almost-horizontal σ_1 trending N336°E and plunging 9°; the value of ratio Φ (0.953) indicates that σ_1 and σ_2 are of similar magnitude; quality factor n_1 is 0 while n_2 is of only 3.

– The state of stress determined for 8 mechanisms of the 1994 seismic crisis is strike-slip with almost-horizontal σ_1

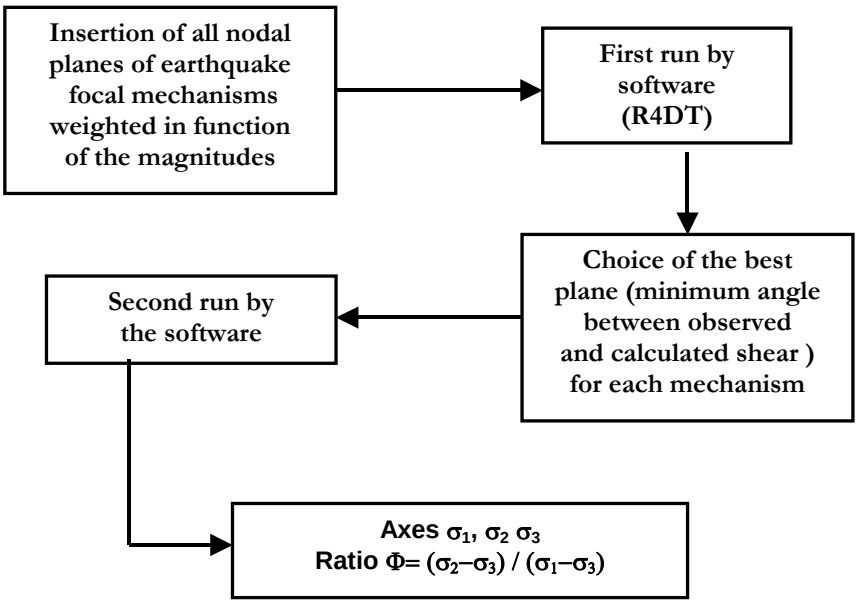

Figure 6. Methodology of determination of the parameters of the main stress axes and ratio Φ with the help of program Tensor.

Table III. Parameters of the state of stress calculated for the events of the Al Hoceima area represented by the azimut and plunge of the main maximal (σ_1) and minimal (σ_3) compressive stress, and the stress ratio Φ (=σ_2–σ_3/σ_1–σ_3). N, number of events selected for the final calculation (second run of R4DT program).

set	N	σ_1		σ_3		Φ	n_1	n_2
		Az.	Pl.	Az.	Pl.			
Isolated	13	336	09	245	03	0.953	0	3
1994 crisis	8	140	19	042	20	0.22	3	4
2004 crisis	16	326	01	056	04	0.3	0	0

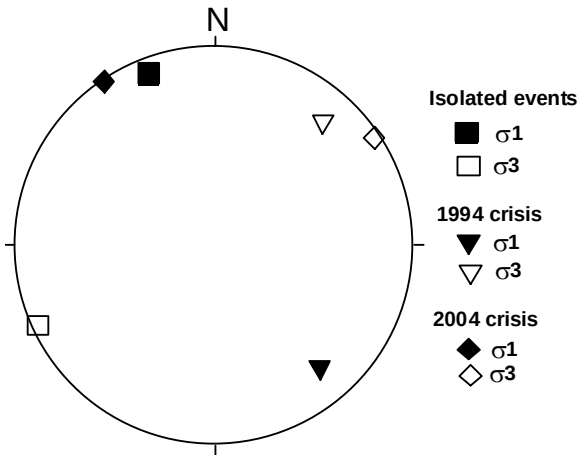

Figure 7. Plot of the main maximal (σ_1) and minimal (σ_3) stress axes (equal area, lower hemisphere). See Table III for the numerical results.

and σ_3 trending N140°E and N042°E respectively (Table III) ; ratio Φ is 0.22 ; quality factor n_1 is 3 while n_2 is of 4.

– Finally, the state of stress for the 2004 crisis, determined with the help of 16 mechanisms calculated by IGN, correspond to a strike-slip regime with σ_1 trending N326°E and plunging 01 ; σ_3 trending N056°E and plunging 04°; ratio Φ is of 0.3; quality factors n_1 and n_2 are null, which means a very good solution.

Among the determined solutions, single events show solutions that can be considered as very reliable, with the exception of mechanisms 8, 9 and 10, which are of lesser reliability because of the small number of stations used. The other groups of solutions are generally very reliable.

DISCUSSION: REGIONAL STATE OF STRESS IN THE AL HOCEIMA AREA

As extensively discussed in a previous paper (Medina 1995), it can be admitted on the basis of seismotectonic studies (e.g. Carey-Gailhardis & Mercier 1992) that large to moderate earthquakes are related to the *regional* state of stress (i.e. plate and microplate motions), while micro-earthquakes only reflect a *local* state of stress (i.e. block adjustments). On the other hand, it clearly appears from analysis of other attempts of determination of the state of stress (Henares *et al.* 2003, Buforn *et al.* 2004) that obtaining an accurate state of stress strongly depends on the choice of the focal mechanisms. Thus, a heterogeneous population of solutions often leads to poor results because it may generally involve two or more states of stress. Therefore, the best determinations appear to be those that

only take into account a main shock and its largest aftershocks.

The states of stress obtained for the three sets of moderate to large earthquakes (isolated, 1994 and 2004) show similar solutions reflecting a strike-slip regime, with σ_1 and σ_3 horizontal and trending NNW-SSE (N140°E to N156°E) and ENE-WSW (N42°E to N65°E) respectively. The strike differences may be interpreted as due to the iteration procedure and should not be understood to represent temporal rotations of the stress axes. However, ratio Φ for the set of single earthquakes (close to 1; i.e. $\sigma_2 \approx \sigma_1$) is different than those of the seismic sequences (close to 0; $\sigma_2 \approx \sigma_3$). This can be easily explained by the less homogeneous population of mechanisms of the single events, and by the wider area considered. The fault population used for the determination of the state of stress includes normal and strike-slip mechanisms determined on relatively distant fault segments which may have acted independently.

For micro-earthquakes (shocks of magnitude 1 to 3), the state of stress is extensional in the Imzouren area and strike-slip elsewhere (Medina 1995). The state of stress in Imzouren reflects a permutation of σ_1 and σ_2 due to normal faulting along the western fault of the Nekor graben. However, this dataset still needs applying a numerical methodology in order to improve the determination of the state of stress.

For single events, focal mechanisms located in the Alboran sea all show a strong normal component; however, numerous other teleseisms and microseisms located onshore also show normal faulting mainly; therefore, the type of mechanisms does not *a priori* seem to be related to the location of the events.

The three states of stress are somewhat different from those obtained by Henares *et al.* (2003), and closer to that determined by Buforn *et al.* (2004).

From isolated shallow events (h<40 km) in a larger area comprising Al Hoceima and Nador (their sector 2; approx. 4.5°W-1.5°W), Henares *et al.* (2003) obtained two states of stress using the right dihedra method: (i) for large earthquakes (m_b 5.3-5.7), compression is horizontal and N55°-90°E, while extension is also horizontal and N0°-35°E; (ii) for moderate earthquakes (mb 4.0-4.6), compression is N25°W dipping NNW, while extension is N55°-90°E dipping ENE.

In the Rif–Betics–Alboran area, Buforn *et al.* (2004; their sector B) obtained from total seismic moment tensor calculations a strike-slip regime with a small normal component. The data set comprises shallow (h<40 km), large to moderate earthquakes (mb≥5 for shocks before 1975, and mb≥4.0 after 1975). Axis *P* trends NW-SE with a small dip towards NW, while axis *T* is horizontal and NE-SW.

Although different, the solutions we obtained are in agreement with those of Henares *et al.* (2003) for large earthquakes, and Buforn *et al.* (2004). Our results show a good fit with the plate displacement vector, the trend of which is N320°E in the Al Hoceima area (models NUVEL-1 et NUVEL-1A). This trend is also in agreement with the NW-SE compressional stress active in Plio-Quaternary times. However, it is slightly oblique to the plate displacement vector determined from geodesy (McClusky *et al.* 2003), which is oriented N116E (N296).

However, it should be noted that this state of stress only applies to the Al Hoceima area and should not be extended westwards to the rest of the Rif chain, as the latter is submitted to a complex regime involving extension and especially lateral escape of fault-delimited blocks (Chalouan *et al.* 2004).

CONCLUSIONS

(1) In the Al Hoceima area, focal mechanisms are homogeneous by event (main shock and its aftershocks), but become heterogeneous when corresponding to single events which are time- and space-distant, reflecting the structural diversity of the area.

(2) The NW-SE trend of the main compressional stress axis agrees with the displacement vector of Africa with respect to Eurasia in the area, with local variations.

(3) The obtained states of stress correspond to the regional state of stress for moderate earthquakes (M≥4) and to local states of stress for the weak events.

Acknowledgements

This paper has been presented as a communication to the International Conference on the Al Hoceima earthquake of 2004, held at Al Hoceima (24-26 February 2005). We are grateful to Pr. Elisa Buforn (Universidad Complutense, Madrid) and to Pr. Jesus Galindo-Zaldivar (Universidad de Granada) for critical reviews which helped improving the first draft of the manuscript.

Références

Allmendinger R.W., Marrett R.A. & Cladouhos T. 1989. Fault Kinematics version 2.0 a program for analyzing fault slip data. (unpublished document).

Angelier J. 1990. Inversion of field data in fault tectonics to obtain the regional stress – III. A new rapid direct inversion method by analytical means. *Geophys. J. Int.,* 103, 363-376.

Angelier J. & Goguel J. 1979. Sur une méthode simple de détermination des axes principaux des contraintes pour une population de failles. *C.R. Acad. Sci. Paris* 288, sér. D, 307-310.

Angelier J. & Mechler P. 1977. Sur une méthode graphique de recherche des contraintes principales également utilisable en tectonique et en séismologie: la méthode des dièdres droits. *Bull. Soc. géol. Fr.*, (7), XIX, 6, 1309-1318.

Bezzeghoud M. & Buforn E. 1999. Source parameters of the 1992 Melilla (Spain, Mw=4.8), 1994 Alhoceima (Morocco, Mw=5.8) and 1994 Mascara (Algeria, Mw=5.7) earthquakes and seismotectonic implications. *Bull. Seismol. Soc. Am.,*89, 359-372.

Buforn E., Bezzeghoud M., Del Fresno C., Borges F.J., Madariaga R., Pro C. & Martin-Davila 2005. Etude du processus de rupture du séisme d'Alhoceima (24/02/2004, Mw=6.2) à partir des données régionales et télésismiques. *Coll. Intern. « Séisme d'Al Hoceima : bilan et perspectives »*, Al Hoceima, 24-26 février 2005, p. 26.

Buforn E., Bezzeghoud M., Udias A. & Pro C. 2004. Seismic sources on the Iberia-African plate boundary and their tectonic implications. *Pure appl. Geophys.,* 161, 3, 623-646.

Calvert A., Gomez F., Seber D., Barazangi M., Jabour N., Ibenbrahim A.& Demnati A. 1997. An integrated geophysical investigation of recent seismicity in the Al-Hoceima region of north Morocco. *Bull. Seismol. Soc. Amer*., 87, 3, 637-651.

Carey E. & Brunier B. 1974. Analyse théorique et numérique d'un modèle mécanique élémentaire appliqué à l'étude d'une population des failles. *C.R. Acad. Sci. Paris,* 279, sér. D, 397-400.

Carey-Gailhardis E. & Mercier, J.-L. 1987. A numerical method for determining the state of stress using focal mechanisms of earthquake populations: application to Tibetan teleseisms and microseismicity of Southern Peru. *Earth & Planet. Sci. Letters* 82, 165-179.

Carey-Gailhardis E. & Mercier J.L. 1992. Regional state of stress, fault kinematics and adjustments of blocks in a fractures body of rock: application to the microseismicity of the Rhine graben. *J. Struct. Geol*., 14, 8/9, 1007-1017.

Chalouan A., Galindo-Zaldivar, J., Bargach, K., Ruano P., Akil M., Chabli A., Marin-Lechado C., Ahmamou M., Sanz de Galdeano C., Gourari L., Ben Makhlouf M. & Azzouz O. 2004. Evolution tectonique plio-quaternaire du front de la chaîne du Rif et de son avant-pays meseto-atlasique : un modèle en coins expulsés vers le SW. *Coll. Intern. « Séisme d'Al Hoceima : bilan et perspectives »,* Al Hoceima, 24-26 février 2004, p. 15.

Cherkaoui T.-E. 1988. Fichier des séismes du Maroc et des régions limitrophes 1901-1984. *Trav. Inst. Sci.,* Rabat, sér. Géol. & Géogr. phys., 17, 158 p.

Cherkaoui T.-E., Hatzfeld D., Jebli H., Medina F. & Caillot V. 1990. Etude microsismique de la région d'Al Hoceima. *Bull. Inst. Sci*., Rabat, 14, 25-34.

Chotin P. & Aït Brahim L. 1988. Transpression et magmatisme au Néogène-Quaternaire dans le Maroc oriental. *C. R. Acad. Sci. Paris*, 306, sér. II, 1479-1485.

DeMets C., Gordon R.G., Argus D.F. & Stein S. 1994. Effect of the recent revisions to the geomagnetic reversal time scale on the estimate of current plate motions. *Geophys. Res. Lett.*, 21, 2191-2194.

Dorbath L., Hahou Y., Delouis B., Dorbath C., Van Der Woerde J., Badrane S., Frogneux M., Haessler H., Jacques E. Menzhi M. & Tapponnier P. 2005. Etudes sismologiques sur le séisme d'Al Hoceima : localisation et mécanisme du choc principal et des répliques, contraintes et structure de la zone épicentrale. *Coll. Intern. « Séisme d'Al Hoceima : bilan et perspectives »,* Al Hoceima, 24-26 février 2005, p. 22.

El Alami S.O., Tadili B., Cherkaoui T.-E., Medina F., Ramdani M., Aït Brahim L. & Harnafi M. 1998. The Al Hoceima earthquake of May, 26, 1994 and its aftershocks : a seismotectonic study. *Ann. Geofis.,* 41, 519-537.

El Alami S.O., Tadili B., Aït Brahim L. & Mouayn I. 2004. Seismicity of Morocco for the period 1987-1994. *Pure appl. Geophys.*, 161, 969-982.

Elmrabet T. 2005. *Les tremblements de terre majeurs dans la région du Maghreb, et leurs conséquences sur l'homme et l'environnement.* Ed. CNRST-LAG, Rabat, 478 p. [in Arabic]

Etchecopar A., Vasseur G. & Daignières M. 1981. An inverse problem in microtectonics for the determination of stress tensors from fault striation analysis. *J. Struct. Geol*., 3, 1, 51-65.

Frizon de Lamotte D. 1982. Contribution à l'étude de l'évolution structurale du Rif oriental. *Notes & Mém. Serv. géol. Maroc*. 314, 239-309.

Frohlich C. & Apperson K.D. 1992. Earthquake focal mechanisms, moment tensors, and the consistency of seismic activity near plate boundaries. *Tectonics,* 11, 2, 279-296.

Galindo-Zaldivar J., Gonzalez-Lodeiro F. & Jabaloy A. 1993. Stress and paleostress in the Betic-Rif Cordilleras (Miocene to present). *Tectonophysics*, 227, 105-126.

Groupe de Recherche Néotectonique de l'Arc de Gibraltar 1977. L'histoire tectonique récente de l'Arc de Gibraltar. *Bull. Soc. géol. Fr*., (7), XIX, 3, 591-605.

Guillemin M. & Houzay J.P. 1982. Le Néogène post-nappe et le Quaternaire du Rif nord-oriental. Stratigraphie et tectonique des bassins de Melilla, du Kert, de Boudinar et du piedmont des Kebdana. *Notes & Mém. Serv. géol. Maroc,* 314, 7-239.

Hatzfeld, D. 1978. *Etude sismotectonique de la zone de collision ibéro-maghrébine*. Thèse d'Etat, Univ. Grenoble, 281 p.

Hatzfeld D., Caillot V., Cherkaoui T.-E., Jebli H. & Medina F. 1993. Microearthquake seismicity and fault plane solutions study around the Nékor strike-slip fault, Morocco. *Earth & Planet. Sci. Letters,* 120, 31-41.

Henares J., Lopez Casado C., Sanz de Galdeano C., Delgado J. & Pelaez J.A. 2003. Stress fields in the Iberian-Maghrebi region. *J. Seismol.*, 7, 65-78.

Leblanc D. & Olivier P. 1984. Role of strike-slip faults in the Betic-Rifian orogeny. *Tectonophysics,* 101, 345-355.

McClusky S., Reilinger R., Mahmoud S., Ben Sari D. & Tealeb A. 2003. GPS constraints on Africa (Nubia) and Arabia plate motions. *Geophys. J. Int.,* 155, 126-138.

Medina F. 1995. Present-day state of stress in northern Morocco from focal mechanism analysis. *J. Struct. Geol*., 17, 1035-1046.

Medina F. & Cherkaoui T.-E. 1992. Mécanismes au foyer des séismes du Maroc et des régions voisines (1901-1986). Implications tectoniques. *Eclogae Geol. Helv*., 85, 2, 433-457.

Mourier Th. 1982. *Etude géologique et structurale du Massif des Bokkoya (Rif oriental, Maroc).* Thèse de 3ème cycle, Univ. Paris XI, Orsay, 300 p.

Rivera L. & Cisternas A. 1990. Stress tensor and fault plane solution for a population of earthquakes. *Bull. Seismol. Soc. Am.*, 80, 600-614.

Rueda J. & Mezcua J. 2004. Determinacion del tensor momento sismico en tiempo real. Primeros resultados en España. Instituto Geografico Nacional, Madrid, 60 p.

Stich D. Morales J., Mancilla F. & Alguacil G. 2003. Moment tensor determination for the Ibero-Maghrebian region. *Orfeus Newslett.,* 5, 2, 1-9.

Thauvin S. 1971. La zone rifaine. *In*. Serv. géol. Maroc (edit) *Ressources en eau du Maroc*. Tome I: Domaines du Rif et du Maroc oriental. *Notes & Mém. Serv. géol. Maroc,* 231, 69-79.

Udias A., Lopez-Arroyo A. & Mezcua J. 1976. Seismotectonic of the Azores-Gibraltar region. *Tectonophysics* 31, 259-289.

Wells D.L. & Coppersmith K.J. 1994. New empirical relationships among magnitude, rupture length, rupture width, rupture area, and surface displacement. *Bull. Seismol. Soc. Am.,* 84, 6, 974-1002.

Addendum

During editorial procedure of the present paper, several new papers on the Al Hoceima event of 2004 were published. These studies used InSAR interferometry and/or waveform analysis (Cakir *et al.* 2006, Biggs *et al.* 2006), moment tensor inversion (Stich *et al*. 2005), or GPS data (Fadil *et al.* 2006). However, in order to respect the original text of the 2005 presentation, their data have not been taken into account in the present paper.

Biggs J., Bergman E., Emmerson B., Funning J.G., Jackson J. Parsons B. & Wright T.J. 2006. Fault identification for buried strike-slip earthquakes using InSAR: The 1994 and 2004 Al Hoceima, Morocco earthquakes. *Geophys. J. Internat*., 166, 1347-1362.

Cakir Z., Meghraoui M., Akoglu A.M., Jabour N., Belabbes S. & Aït Brahim L. 2006. Surface deformation associated with the Mw 6.4, 24 February 2004 Al Hoceima, Morocco, earthquake deduced from InSAR: implications for the active

tectonics along North Africa. *Bull. Seismol. Soc. America*, 96, 1, 59-68.

Fadil A., Vernant P., McClusky S., Reilinger R., Gomez F., Ben Sari D., Mourabit T., Feigl K. & Barazangi M. 2006. Active tectonics of the western Mediterranean : geodetic evidence for rollback of a delaminated subcontinental lithospheric slab beneath the Rif Mountains, Morocco. *Geology,* 34, 7, 529-532.

Stich D., Mancilla F., Baumont D. & Morales J. 2005. Source analysis of the Mw 6.3 2004 Al Hoceima earthquake (Morocco) using regional apparent source time functions. *J. Geophys. Res.,* 110, B06306, doi:10.1029/2004/B003366, 2005.

Manuscript received 17 April 2006
Revised version accepted 18 October 2006

Appendix

Table A. Focal parameters and mechanisms of isolated events used in this study.

N°	Date	Time	Lat. (N)	Long. (W)	Magnitude	Depth	Type	Plane A (tr., dip, rake)	Plane B (tr., dip, rake)	Axis *P*	Axis *T*	*N*	Ref
1	17/04/1968	09-12-04	35.24	3.73	5	13	FM	348; 82;**[*1]	80; 80; –8	304; 12	35; 02	40 (10)	H78
2	30/10/1968	11-41-57	35.28	3.76	4.6	NC	FM	286; 55; 145	38; 62; 40	160[2]; 04	254; 46	n	CB94
3	07/04/1970	09-16-14	34.87	3.90	4.8	27	FM	244; 64; 155	346; 70; 19	114; 03[3]	205; 35 [3]	17 (2)	H78
4	29/04/1973	14-37-57	34.63	4.17	4.5	35	FM	32; 90; 0	122; 90; 0	167; 0	77; 0	27 (4)	H78
5	14/07/1974	02-55-26	35.58	3.68	4.3	2	FM	36; 90; 0	126; 90; 0	351; 0	81; 0	13 (3)	H78
6	15/07/1977	05-41-50	35.17	3.73	3.7 (ISC)	17	FM	211; 70; –25	310; 66; –158	170; 32	262; 03	11 (1)	MC92
7	24/02/1979	21-19-23	34.93	4.28	4.3	5	FM	51; 40; –23	159; 75; –129	32; 46	276; 23	12 (0)	MC92
8	21/04/1979	19-52-06	35.03	4.00	3.8	5	FM	171;70; 32	71; 60; 158	300; 07	35; 36	9 (1)	M95
9	20/03/1981	14-08-00	35.13	3.90	3.9	5	FM	168; 80; 37	70; 54; 168	294; 17	034; 32	9 (1)	M95
10	07/04/1981	23-37-00	35.11	3.98	3.7	5	FM	183; 75; 33	85; 60; 163	310; 10	047; 33	8 (1)	M95
11	09/12/1987	23-14-26	35.41	3.81	4.3 (m_b)	7	FM	54; 49; –58	190; 50; –123	38; 64	303; 08	N	HN03
12	05/10/1988	00-42-11	35.50	3.88	4	11	FM	248; 26; –58	32; 68; –105	280; 64	136; 22	28 (9)	IGN88
13	20/10/1998	23-47-03	34.84	3.77	3.9 (Mw)	NC	MT	116; 54; –118	338; 44; –56	328; 67	225; 05		IAG
14	18/07/1999	17-26-47	35.24	4.09	3.9 (Mw)	NC	MT	118; 83; –149	24; 59; –7	346; 26	247; 16		IAG
15	08/06/2001	13-47-32	35.49	3.93	4 (Mw)	NC	MT	128; 71; –157	30; 68; –20	349; 29	259; 02		IAG

References: H78: Hatzfeld 1978; CB94: Coca & Buforn 1998; MC92: Medina & Cherkaoui 1992; M95: Medina 1995; HN03: Henares *et al.* 2003; IGN88: Instituto Geografico Nacional, Madrid 1988; IAG: Instituto Andaluz de Geofisica.

Types of mechanism: FM: first motion of P-waves; MT: moment tensor inversion.

N: number of stations used (in parentheses number of incompatible motions).

Table B. Parameters of the focal mechanism of the main earthquake of 1994 according to various sources. (WFA: waveform analysis; CMT: centroid moment tensor)

Plane A str. dip (°)	**Plane B str.(°) dip (°)**	**P-axis az. (°) pl.(°)**	**T-axis az.(°) pl.(°)**	**Reference**
93 75	00 80	316 18	47 04	USGS (P-Waves)
93 80	02 84	317 11	47 03	USGS (M-Tensor)
112 48	17 85	326 33	72 24	HARVARD (CMT)
91 83	00 87	316 14	224 04	HARVARD (P-waves)
291 86	200 79	156 11	67 05	EMSC
202 60	100 72	151 04	59 30	El Alami *et al*. 1998 (P-waves)
329 77		281 40	28 19	Bezzeghoud & Buforn 1999 (WFA)
355 69		311 13	218 16	Bezzeghoud & Buforn 1999 (WFA)

Table C. List of focal mechanisms related to the 1994 crisis (after El Alami *et al* 1998). Abbreviations as for Table A.

Date	**Time**	**Lat. N**	**Long. W**	**Depth**	**Mag.**	**Plane A**		**Plane B**		**Axis P**		**Axis T**		**N**
						Tr.	**Dip**	**Tr.**	**Dip**	**Az**	**Pl**	**Az**	**Pl**	
26/05/94	12-27-54	35°12'	4°01'	20	4.4	185°	70°	298°	44°	140°	49°	247°	15°	13(1)
28/05/94	03-32-02	35°14'	4°03'	10	3.5	180°	50°	308°	54°	159°	60°	063°	03°	10(1)
29/05/94	19-14-05	35°14'	4°02'	10	3.3	220°	80°	316°	60°	174°	29°	270°	19°	11(3)
29/05/94	23-45-06	35°16'	4°02'	10	4.0	199°	82°	296°	56°	146°	37°	254°	23°	11(1)
01/06/94	00-53-52	35°11'	4°01'	8.5	4.0	209°	64°	330°	43°	166°	55°	273°	13°	11(1)
03/06/94	08-57-38	35°11'	4°02'	8	4.6	190°	55°	082°	66°	138°	07°	040°	44°	21(5)
08/06/94	03-08-31	35°11'	4°02'	10	3.6	008°	80°	100°	80°	324°	14°	234°	01°	11(1)

Table D. Parameters of the focal mechanism of the main earthquake of 2004 according to various sources.

Plane A str. dip rake °	**Plane B str. dip rake°E**	**P-axis az. (°) pl.(°)**	**T-axis az.(°) pl.(°)**	**Reference**
21 86 –19	111 89 –176	336 04	246 03	USGS
18 81 –29	113 61 –170			Harvard
208 67 07	115 84 157	163 11	069 20	SED
198 73 –37	300 55 –159	154 37	253 12	INGV

Table E. List of focal mechanisms of the 2004 crisis (after IGN) used for the present study. Mo: scalar moment; Q: quality of solution according to IGN.

N° IGN	Date	Time	Lat. N	Long. W	Mw	Depth (km)	Mo	Plane A (tr., dip, rake)	Plane B (tr., dip, rake)	Q
458391	24/02/2004	02-27-46	35.142	3.997	6.2	6	2.66E+25	200 82 023	107 67 171	3
459905	25/02/2004	05-21-14	35.121	3.931	4.5	9	6.35E+22	098 88 176	188 86 002	3
460103	25/02/2004	12-44-54	35.052	3.861	5.2	6	6.54E+23	202 74 036	101 56 161	3
460255	25/02/2004	16-33-28	35.170	3.941	4.0	9	1.09E+22	293 85 162	025 72 005	3
460715	26/02/2004	12-07-03	35.190	4.064	4.8	9	1.94E+23	197 86 008	107 82 176	3
461000	27/02/2004	00-59-00	35.139	3.990	4.3	3	2.84E+22	285 88 –178	195 88 –002	4?
461386	27/02/2004	16-50-42	35.184	3.919	4.5	15	5.85E+22	098 78 164	191 75 013	4
461723	28/02/2004	16-29-25	35.023	4.013	4.2	6	2.10E+22	255 63 102	050 29 068	3
462848	02/03/2004	20-36-26	35.148	3.867	4.4	6	3.78E+22	198 89 029	108 61 179	4
463533	04/03/2004	11-44-14	35.165	3.987	3.8	12	4.87E+21	102 82 171	193 81 008	4
464446	07/03/2004	06-37-52	35.060	4.005	5.0	12	3.28E+23	272 87 –176	182 86 –003	3
464584	07/03/2004	10-30-05	35.115	3.893	3.5	33	2.19E+21	189 84 016	98 74 174	2
466339	12/03/2004	17-21-51	34.921	4.051	4.8	9	1.88E+23	345 48 –073	140 45 –108	4
468390	18/03/2004	11-45-31	35.165	4.225	3.9	9	8.36E+21	073 50 120	210 48 059	2
469073	20/03/2004	09-37-26	35.007	4.148	4.5	9	6.65E+22	114 87 –171	024 81 –003	4
474163	06/04/2004	01-53-09	35.060	4.111	4.2	6	2.01E+22	277 56 129	041 50 046	3
487009	23/05/2004	00-29-45	35.157	4.015	3.7	24	4.48E+21	099 77 165	193 75 014	3
494264	20/06/2004	22-47-05	34.936	3.875	4.3	24	3.30E+22	289 83 –170	198 80 –008	3
515511	10/10/2004	08-13-58	35.045	3.983	3.9	9	9.02E+21	176 86 004	085 86 176	2